

NOPE: Novel Object Pose Estimation from a Single Image

Van Nguyen Nguyen¹, Thibault Groueix², Yinlin Hu³, Mathieu Salzmann⁴, Vincent Lepetit¹
¹LIGM, Ecole des Ponts, ²Adobe, ³MagicLeap, ⁴EPFL

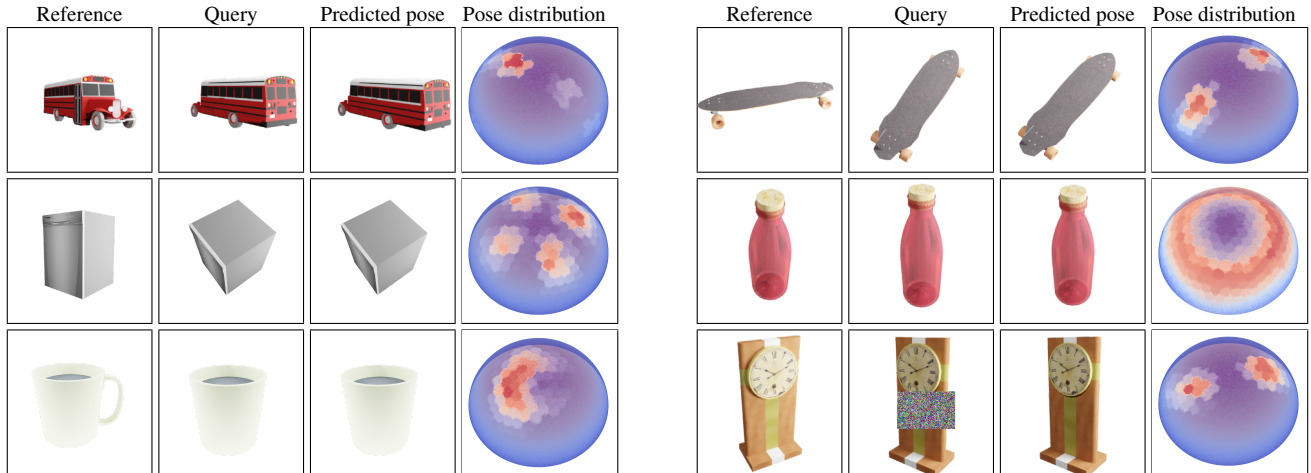


Figure 1. Given as input a single reference view of a novel object, our method predicts the relative 3D pose of a query view and its ambiguities. **We visualize the predicted pose by rendering the object from this pose, but the 3D model is only used for visualization purposes, not as input to our method.** Our method works by estimating a probability distribution over the space of 3D poses, visualized here on a sphere centered on the object. **We use the canonical pose of the 3D model to visualize this distribution, but not as input to our method.** From this distribution, we can also identify the pose ambiguities: For example, in the case of the bottle, any pose with the same pitch and roll is possible; in the case of the mug, a range of poses are possible as the handle is not visible in the query image. Our method is also robust to partial occlusions, as shown on the clock hidden in part by a rectangle in the query image.

Abstract

The practicality of 3D object pose estimation remains limited for many applications due to the need for prior knowledge of a 3D model and a training period for new objects. To address this limitation, we propose an approach that takes a single image of a new object as input and predicts the relative pose of this object in new images without prior knowledge of the object’s 3D model and without requiring training time for new objects and categories. We achieve this by training a model to directly predict discriminative embeddings for viewpoints surrounding the object. This prediction is done using a simple U-Net architecture with attention and conditioned on the desired pose, which yields extremely fast inference. We compare our approach to state-of-the-art methods and show it outperforms them both in terms of accuracy and robustness. Our source code is publicly available at <https://github.com/nv-nguyen/nope>.

1. Introduction

Estimating the 3D pose of objects has seen significant progress in the past decade with regard to both robustness and accuracy [12, 16, 33, 47, 57]. Specifically, there has been a considerable increase in robustness to partial occlusions [8, 29, 30], and the need for large amounts of real annotated training images has been relaxed through the use of domain transfer [1], domain randomization [14, 44, 48], and self-supervised learning techniques [46] that leverage synthetic images for training.

Unfortunately, the practicality of 3D object pose estimation remains limited for many applications, including robotics and augmented reality. Typically, existing approaches require a 3D model [15], a video sequence [6, 43], or sparse multiple images of the target object [58] (to ref-

erence only the most recent works), and a training stage. Several techniques aim to prevent the need for retraining by assuming that new objects fall into a recognized category [5, 51], share similarities with the previously trained examples as in the T-LESS dataset [44], or exhibit noticeable corners [31].

In this paper, we introduce an approach, which we call **NOPE** for **Novel Object Pose Estimation**, that only requires a single image of the new object to predict the relative pose of this object in any new images, without the need for the object’s 3D model and without training on the new object. This is a very challenging task, as, by contrast with the multiple views used in [43, 58] for example, a single view only provides limited information about the object’s geometry.

To achieve this, we train NOPE to generate novel views of an object. These novel views can be used as ‘templates’ annotated with the corresponding poses. Matching these templates with new input views lets us estimate the object relative pose with respect to the initial view. Our approach relates to the recent development in novel view synthesis. However, we take this one step further: Motivated by the good performance of recent template matching work for pose estimation [28, 40], instead of predicting plain color images, we directly predict discriminative embeddings of the views. Specifically, our embeddings are extracted by passing the input image through a U-Net architecture with attention and conditioned on the desired pose for the new view.

In essence, in contrast to existing novel view synthesis works [24, 32], for our pose estimation task, we do not need to create a 3D model of the object. This saves significant computation time, as optimizing a 3D model using a single view takes at least one hour [62] or longer [54]. By contrast, our approach based on direct inference of the view embeddings is extremely fast, processing an image in less than 2 seconds. Yet, it yields accurate pose estimates with more than 65% accuracy on average on unseen instances or categories. Our work is also related to motion prediction between 2 images, such as [27, 49], which predict the camera displacement between two images. Our comparisons to the closest work to ours [27] show that we significantly outperform this approach.

Furthermore, we show that our approach can identify the pose ambiguities due, for example, to symmetries [20], even if we do not have access to the object 3D model but only to a single view. To this end, we estimate the distribution over all poses for the query, which becomes increasingly less peaked as the pose suffers from increasingly many ambiguities. Figure 1 depicts a variety of ambiguous and unambiguous cases with their pose distributions.

In summary, our main contribution is to show that we can efficiently and reliably recover the relative pose of an unseen object in novel views given only a single view of

that object. To the best of our knowledge, our approach is the first to predict ambiguities due to symmetries and partial occlusions of unseen objects from only a single view.

2. Related work

In this section, we first review various approaches to novel view synthesis. We then shift our focus to pose estimation techniques that aim to achieve generalization.

2.1. Novel view synthesis from a single image

Our method generates discriminative feature views, which are conditioned on a reference view and the relative pose between the views. This relates to the pioneering work of NeRFs [25] since it performs novel-view synthesis. While recent advancements have improved the speed of NeRFs [26, 39, 55], our approach is still orders of magnitude faster as it does not require the creation of a full 3D volumetric model. Furthermore, our approach only requires a single input view, whereas a typical NeRF setup necessitates around 50 views. Reducing the number of views required for NeRF reconstruction remains an active research area, especially in the single-view scenario [24, 56].

Recent works [24, 62] have had successes generating novel views via NeRFs using a sparse set of views as input by leveraging 2D diffusion models. For images, the breakthrough in diffusion models [7, 41] have unlocked several workflows [35, 37, 38]. For 3D applications, DreamFusion [32] pioneered a score-distillation sampling that allows for the use of a 2D diffusion model as an image-based loss, leveraged by 3D applications via differentiable rendering. This has resulted in significant improvements for tasks previously trained with a CLIP-based image loss [9, 10, 13, 17, 34, 50]. By building on top of score-distillation sampling, SparseFusion [62] reconstructs a NeRF scene with as few as two views with relative pose, while the concurrent work RealFusion [24] does it from a single input view, although the reconstruction time is impractical for real-time applications. Our approach is much faster as we do not create a 3D representation of the object.

Closest to our work, 3DiM [52] generates novel views of an object by conditioning a diffusion model on the pose. Instead of leveraging foundation diffusion models in 2D like DreamFusion does, they retrain a diffusion model specifically for this task. While they have not applied their approach to template-based pose estimation, we design such a baseline and compare against it. We find that the diffusion model tends to always generate sharp images, even at the cost of sometimes changing the texture or hallucinating wrong details which hinders the performance of the template-based approach. In contrast, our approach generates novel views directly in an embedding space instead of pixel space, which is much more efficient as we will demonstrate in Section 3.1.

Finally, several approaches [22,23] generate novel views by conditioning a feed-forward neural network on the 3D pose, which we also do with a U-Net. We share with those approaches an advantage in speed : such feed-forward neural network are one or two orders of magnitude faster than current diffusion model. However, the way we perform pose estimation is fundamentally different. We use novel-view synthesis in a template-based matching approach [28], while they use it in a regression-based optimization. In practice, we found these methods to work well on a limited number of object categories, and we observed their performance to deteriorate significantly when evaluating on novel categories.

2.2. Generalizable object pose estimation

Although many recent methods for estimating the 3D pose of an object from an image have shown significant advances in both efficiency and accuracy [2, 14, 30, 42, 44, 45, 53], most of them can only work for known objects, which means they need to be retrained on every new object, limiting their application range.

Several techniques have been explored to generalize better to unseen object pose estimation, such as generic 2D-3D correspondences [31], an energy-based strategy [58], key-point matching [43], or template matching [15, 18, 28, 40, 59]. Despite significant progress, these methods either need an accurate 3D model of the target or they rely on multiple annotated reference images from different viewpoints. These 3D annotations are challenging to obtain in practice. By contrast, we propose a strategy that works with neither the 3D model of the target nor the annotation of multiple views. More importantly, our method predicts accurate poses with only a single reference image, and generalizes to novel objects without retraining.

3. Method

3.1. Motivation

To motivate our approach, we evaluate the use of the state-of-the-art 3D model-based image generation method (3DiM) [52] for pose estimation. 3DiM is a diffusion-based method for view synthesis in pixel space. To apply it to pose prediction given a reference image of an object, we experimented with using it to generate a set of novel views from many different viewpoints and match a query image of the object to these views in pixel space. Since the generated views are annotated with the corresponding pose, this gives us a pose estimate.

As shown in Figure 2, the images generated by 3DiM look very realistic. However, the recovered poses are not very accurate. This can be explained in part by the fact that diffusion can “invent” details that disturb image matching. The limitations of this approach will further be quan-

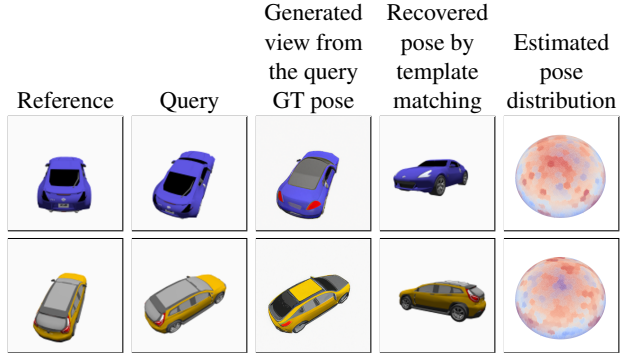


Figure 2. **The limit of image generation with diffusion models for pose prediction.** While the images generated by 3DiM look very realistic, they may change the appearance of the object, impairing the similarity computation between the query image and the generated view, and hence the pose estimation when used for our problem. Notice that the probability distributions does not peak on the right pose but shows many wrong local maxima.

tatively demonstrated in our experiments (Table 1). This motivates us to learn to directly generate a discriminative representation of the views.

In this section, we first motivate our approach with an experiment based on novel view generation. We then describe our architecture, how we train it, and how we use it for pose prediction and for identifying pose ambiguities.

3.2. Framework

Figure 3 gives an overview of our approach. We train a deep architecture to generate embeddings of novel views of an object using pairs of images of objects from a first set of object categories. In practice, we consider embeddings computed with the network of [28], as it was shown to yield a robust representation for template matching. To generate these embeddings, we use a U-Net-like network with a pose conditioning mechanism that is very close to the one introduced in 3DiM [52] and related to the text-to-image mechanism in [36].

More precisely, we first use a Multilayer Perceptron (MLP) to convert the desired relative viewpoint ΔR with respect to the object pose in the reference view to a pose embedding. We then integrate this pose embedding into the feature map at every stage of our U-Net using cross-attention, as described in [36].

Training. At each training iteration, we build a batch composed of N pairs of images, a reference image and another image of the same object with a known relative pose. The U-Net model takes as input the embedding of the reference image and as conditioning the embedding of the relative pose to predict an embedding for the second image. We jointly optimize the U-Net and the MLP by minimizing the

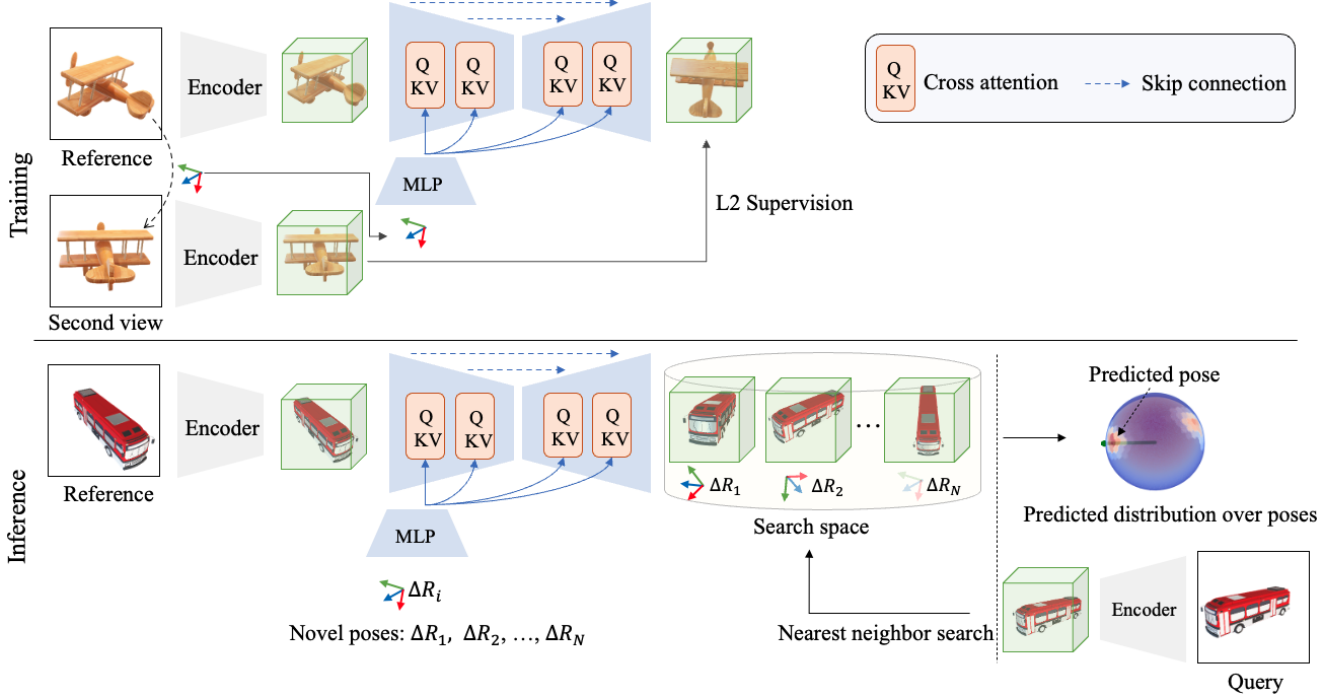


Figure 3. **Overview.** During training, we train a U-Net to predict the embedding of a novel view of an object, given a reference image of the object and a relative pose. The U-Net is conditioned on an embedding of the relative pose computed using an MLP, which we train jointly with the U-Net. At inference, our method first takes as input a reference image of a new object and predicts the embeddings of views of the object under many relative poses. This inference takes around 1 second on a single GPU V100. Then, given a query image of the object, we first compute its embedding and match it against the set of predicted embeddings, which takes about 0.2s. This gives us a distribution over the possible relative poses between the reference and query images. The maximum of the distribution corresponds to the predicted pose.

Euclidean distance between this predicted embedding and the embedding of the query image. Note that we freeze the network of [28] computing the embeddings as it has already been trained.

By training it on a diverse dataset of objects, this architecture generalizes well to novel unseen object categories, as our results will show.

3.3. Pose prediction

Template matching. Once our architecture is trained, we can use it to generate the embeddings for novel views: Given a reference image I_r and a set of N relative viewpoints $\mathcal{P} = (\Delta R_1, \Delta R_2, \dots, \Delta R_N)$, we can obtain a corresponding set of predicted embeddings (e_1, e_2, \dots, e_N) . To define these viewpoints, we follow the approach used in [28]: We start with a regular icosahedron and subdivide each triangle recursively into four smaller triangles twice to get 342 final viewpoints.

Finally, we simply perform a nearest neighbor search to determine the reference point that has the embedding closest to the embedding of the query image. Note that this can be done efficiently [28].

Detecting pose ambiguities. Pose ambiguities arise when the object has symmetries or when an object part that could remove the ambiguity is not visible, as for the mug in Figure 1. By considering the distance between the embedding of the query image and the generated embeddings, we not only can predict a single pose but also identify all the other poses that are possible given the reference and query views.

More formally, we estimate the probability of a relative pose ΔR given reference image I_r and query image I_q as

$$p(\Delta R | I_r, I_q) = \frac{1}{Z} \frac{e_{\Delta R} \cdot e_q}{\|e_{\Delta R}\| \|e_q\|}, \quad (1)$$

where $e_{\Delta R}$ is the embedding predicted by the U-Net from reference image I_r and relative pose ΔR , e_q is the embedding for query image I_q , and Z is a normalization factor. The operator \cdot denotes the dot product.

To illustrate this, we show in Figure 4 three distinct types of symmetry and visualize the pose distribution for corresponding pairs of reference and query images (not shown). The number of regions with high similarity scores is consistent with the number of symmetries and pose ambiguities: If an object has no symmetry, the probability distribution has

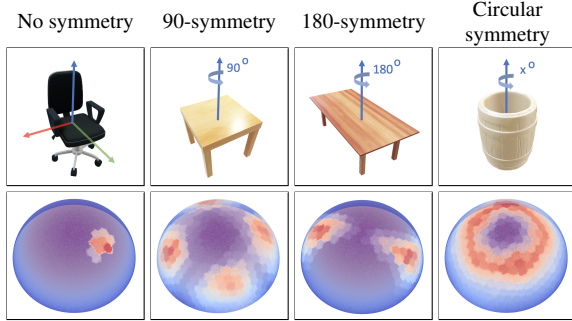


Figure 4. **Object symmetries and the pose ambiguities they may generate**, as estimated by our method given a pair of reference and query images.

a clear mode. The probability distribution for objects with symmetries have typically several modes or even a continuous high-probability region in case of rotational symmetry. We provide additional qualitative results in Section 4.

4. Experiments

In this section, we first describe our experimental setup in Section 4.1, and then compare our method to others ([21, 22, 27, 52]) on both seen and unseen object categories in Section 4.2. Section 4.3 reports an evaluation of the robustness to partial occlusions. In Section 4.4, we conduct an ablation study to investigate the effectiveness of our method in different settings, and finally discuss failure cases of our method in Section 4.6.

4.1. Experimental setup

Dataset. To the best of our knowledge, we are the first method addressing the problem of object pose estimation from a single image when the object belongs to a category not seen during training: PIZZA [27] evaluated on the DeepIM refinement benchmark, which is made of pairs of images with a small relative pose; SSVE [22] and ViewNet [21] evaluated only on objects from categories seen during training.

We therefore had to create a new benchmark to evaluate our method. We created a dataset using the same object categories from ShapeNet [3] as in FORGE [11]. For the training set, we randomly select 1000 object instances from each of the 13 categories as done in FORGE (*airplane, bench, cabinet, car, chair, display, lamp, loudspeaker, rifle, sofa, table, telephone, and vessel*), resulting in a total of 13,000 instances. We build two separate test sets for evaluation. The first test set is the “novel instances” set, which contains 50 new instances that do not appear during training but are still from the object categories used for training. The second test set is the “novel category” set, which includes 100 models from the 10 unseen categories selected

by FORGE (*bus, guitar, clock, bottle, train, mug, washer, skateboard, dishwasher, and pistol*). For each 3D model, we randomly select camera poses to produce five reference images and five query images. We use BlenderProc [4] as our synthetic rendering engine.

Figure 5 illustrates the categories used for training our architecture and the categories used for testing it. The shapes and appearances of the categories in the test set are very different from the shapes and appearances of the categories in the training set and thus constitute a good test set for generalization to unseen categories.

Metrics. We report two different metrics based on relative camera pose error as done in [22]. Specifically, we provide the median pose error across instances for each category in the test set and the accuracy Acc 30 for which a prediction is treated as correct when the pose error is $\leq 30^\circ$. Additionally, we present the results of our method for the top 3 and 5 nearest neighbors retrieved by template matching.

Baselines. We compare our work with all previous methods (to the best of our knowledge) that aim to predict a pose from a single view: PIZZA [27], a regression-based approach that directly predicts the relative pose, and SSVE [22] and ViewNet [21], which employ semi-supervised and self-supervised techniques to treat viewpoint estimation as an image reconstruction problem using conditional generation.

We also compare our method with the recent diffusion-based method 3DiM [52], which generates pixel-level view synthesis. Since 3DiM originally only targets view-synthesis and is not designed for 3D object pose, we use it to generate templates and perform nearest neighbor search to estimate a 3D object pose, as mentioned in Section 3.1. To make 3DiM work in the same setting as us, we retrain it relative pose conditioning instead of canonical pose conditioning.

Only the code of PIZZA is available. The other methods did not release their code at the time of writing, however we re-implemented them. Our numerical results for the “novel instances” cases are similar to the ones reported in the respective papers, which validates our implementations. We use a ResNet18 backbone as in [27] for PIZZA, SSVE, and ViewNet.

We train all models on input images with a resolution of 256×256 except for 3DiM for which we use a resolution of 128×128 since 3DiM performs view synthesis in pixel space, which takes much more memory. Our re-implementations achieve similar performance as the original papers when evaluated on the same data for seen categories, as shown in Table 1, which validates our re-implementation. Our method also uses the frozen encoder from [28] to encode the input images into embeddings of

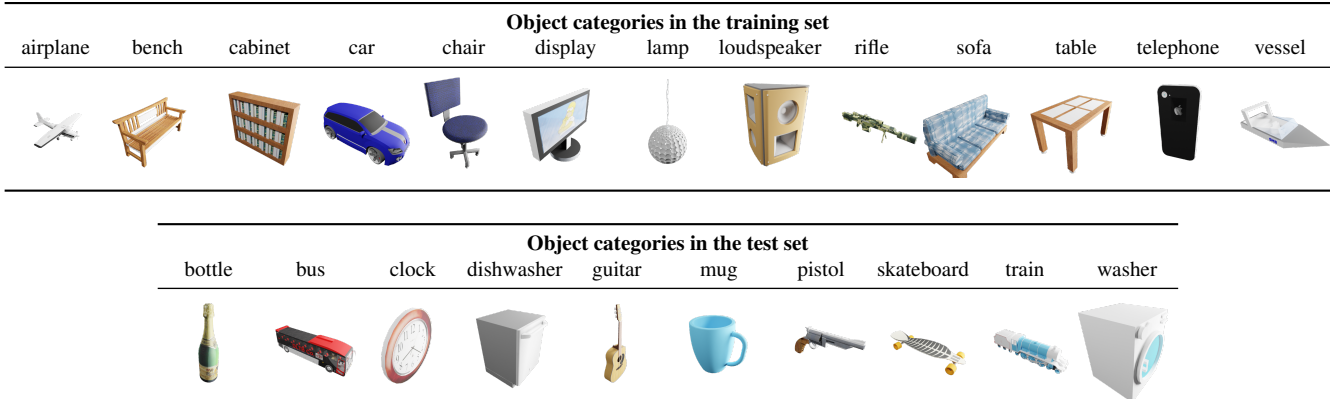


Figure 5. **Training and test sets.** The shapes and appearances in the training and test sets are very different and thus constitute a good test bed for generalization to unseen categories.

	Method	novel inst.	bottle*	bus	clock	dishwasher	guitar	mug	pistol	skateboard	train	washer	mean
Acc 30 \uparrow	ViewNet [21]	80.35	42.46	39.08	35.12	35.13	23.09	50.42	32.13	36.67	51.35	45.03	42.80
	SSVE [22]	78.16	55.59	41.13	53.42	40.03	32.07	57.45	51.03	65.11	48.03	70.69	53.88
	PIZZA [27]	75.16	70.01	41.49	50.13	51.41	16.14	54.69	54.67	61.08	59.45	80.92	55.92
	3DiM [52]	80.13	89.12	46.35	35.17	43.28	21.35	51.12	46.13	53.07	43.57	76.06	53.21
	Ours (top 1)	78.37	90.04	56.49	59.62	66.72	34.31	63.70	83.23	60.58	61.78	80.53	66.85
	Ours (top 3)	91.23	99.04	90.26	78.55	93.59	60.28	75.60	91.23	83.59	83.41	91.83	85.33
	Ours (top 5)	92.97	99.04	94.35	83.23	98.44	66.71	81.85	95.31	89.84	93.57	95.91	90.11
Median \downarrow	ViewNet [21]	6.72	30.56	75.02	18.09	32.07	70.43	36.01	38.04	43.01	26.07	41.39	37.95
	SSVE [22]	6.25	27.63	84.42	19.75	26.17	67.52	34.01	19.25	19.06	24.13	45.13	33.94
	PIZZA [27]	5.95	29.40	65.64	21.03	16.36	60.12	29.92	18.59	22.90	19.59	35.52	29.55
	3DiM [52]	5.86	5.67	59.02	25.15	40.57	55.09	20.07	16.38	18.03	16.82	16.28	25.36
	Ours (top 1)	8.25	5.70	57.64	17.67	13.36	51.52	19.92	8.59	21.10	17.59	5.52	20.62
	Ours (top 3)	5.43	1.07	5.43	8.26	5.50	19.06	11.62	6.41	7.19	7.08	4.28	7.39
	Ours (top 5)	4.64	0.87	4.56	7.45	4.29	15.58	8.83	5.44	5.86	5.10	4.22	6.08

Table 1. **3D pose estimation on novel instances and novel categories from our dataset.** We treat “bottle” as a symmetric category, i.e., the error is only the difference of elevation angle. Since the quality of prediction may depend on the reference image, we report the score as the average of 5 runs with 5 different reference images.

size $32 \times 32 \times 8$. For all methods, we use AdamW [19] with an initial learning rate of $1e-4$. Training takes 10 hours on 4GPUs V100 for each method on average. We refer the reader to the supplementary material for more implementation details.

4.2. Comparison with the state of the art

Table 1 summarizes the results of our method compared with the baselines discussed above. Under both the Acc30 and Median metrics, our method consistently achieves the best overall performance, outperforming the baselines by more than 10% in Acc30 and 10° in Median. In particular, while other works produce reasonable results on unseen instances of training categories, they often struggle to estimate the 3D pose of objects from unseen categories. By contrast, our method works well in this case, demonstrating better generalization ability on unseen categories.

Figure 6 shows some visualization results of our method on unseen categories with and without symmetries. Our method produces more accurate 3D poses than the baselines when a symmetry axis exists.

4.3. Robustness to occlusions

To evaluate the robustness of our method against occlusions, we added random rectangle filled with Gaussian noise to the query images over the objects, in a similar way to Random Erasing [60]. We vary the size of the rectangles to cover a range between 0% to 25% of the bounding box of the object. Figures 1 and 6 show several examples.

Table 2 compares the performance of PIZZA, the best second performing method in our previous evaluation, to our method for different occlusion rates. Our method remains robust even under large occlusions, thanks to the robust discriminative embeddings used to match the images.

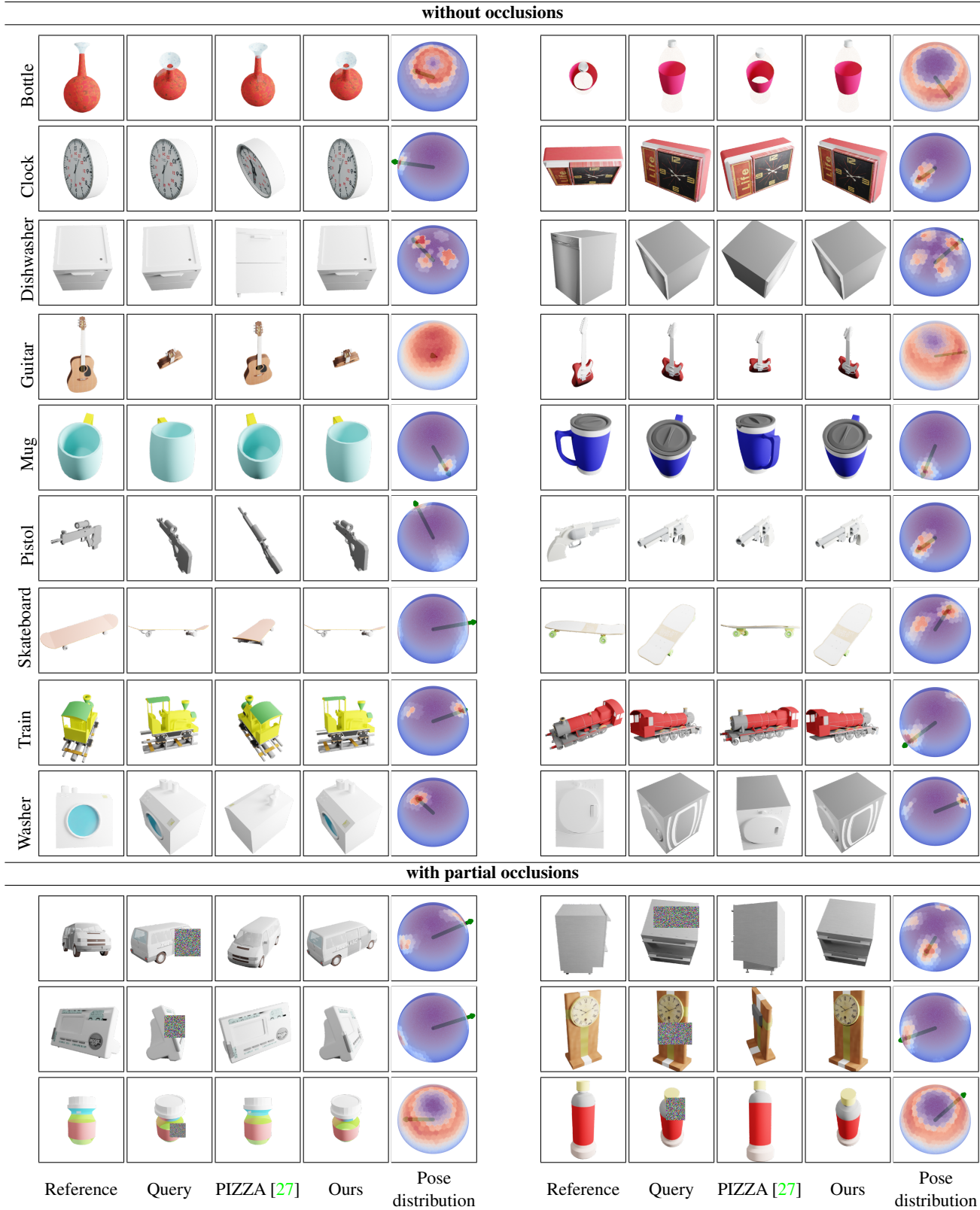


Figure 6. **Visual results on unseen categories** from ShapeNet. An arrow indicates the pose with the highest probability as recovered by our method. We visually compare with PIZZA, which is the method with the second best performance. **We visualize the predicted poses by rendering the object from these poses, but the 3D model is only used for visualization purposes, not as input to our method. Similarly, we use the canonical pose of the 3D model to visualize this distribution, but not as input to our method.**

Method	0%	5%	10%	15%	20%	25%
PIZZA [27]	55.92	51.63	40.32	31.49	25.21	16.58
NOPE (ours)	66.85	61.35	55.42	52.10	50.71	47.52

Table 2. **Robustness to partial occlusions.** We add rectangles of Gaussian noise to the query image, and vary the ratio between the area of the rectangle and the area of the object’s 2D bounding box. We compare with PIZZA, the method with the second best performance in Table 1. Our method remains robust under large occlusions, while PIZZA’s performance decreases significantly.

Method	Memory	Run-time	
		Processing	Neighbors search
3DiM [52]	358.6 MB	13 mins	0.31 s
NOPE (ours)	22.4 MB	1.01 s	0.18 s

Table 3. **Average run-time** of our method and 3DiM [52] on a single GPU V100. We report the memory used for storing novel views, the time taken to generate novel views, and the time taken for nearest neighbor search to obtain the final prediction. Our code is written in plain Pytorch for simplicity and could be further optimized with AITemplate or TensorRT.

In Figure 6, note that our pose probabilities remain peaked on the correct maximum and still shows clear symmetries when they exist.

4.4. Ablation study

Pose conditioning. We experimented with two different pose representations. 3DiM first creates camera rays from a given 3D pose and uses the positional encoding of [25] to obtain a pixel-wise pose condition. This representation is then processed by an MLP before being integrated into the feature map of the U-Net as in our method. We experimented with this method but discovered it does not improve the performance for our problem compared to applying an MLP directly to a representation of the rotation. We favored the second approach for its simplicity.

Rotation representation for the relative pose. Similarly, we experimented with different representations for the rotation: axis-angles, quaternions, and rotation-6D [61]. We observed all these representations yield similar performances, so we use rotation-6D [61] in all of our experiments.

4.5. Runtime analysis

We report the running time of NOPE and 3DiM in Table 3. Our method is significantly faster than 3DiM, thanks to our strategy of predicting the embedding of novel viewpoints with a single step instead of multiple diffusion steps.

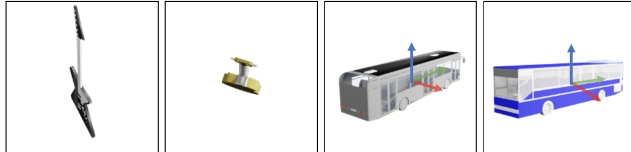


Figure 7. **Failure cases.** “Guitar” objects are barely visible when seen from certain viewpoints, and “bus” and “guitar” objects are nearly symmetrical. This makes the pose estimation very challenging and all the methods perform poorly on these categories.

	Category	ViewNet [21]	SSVE [22]	PIZZA [27]	3DiM [52]	Ours
→	guitar	70.43	67.52	60.12	55.09	51.52
	bus	75.02	84.42	65.64	59.02	57.64
Median	†guitar	31.05	25.46	20.87	20.05	18.65
	†bus	19.26	23.45	17.03	13.25	12.51

Table 4. **Additional experiments on the “guitar” and “bus” categories.** We compare the base results from Table 1 (top) with an evaluation in which we fix the reference viewpoints of the objects from the “guitar” category, and we allow a 180° symmetry in the error metric (bottom with †). We report the median of the errors for each method. The values are significantly better than the values reported in Table 1, which validate the reasons for the poor results on these two categories in the general case.

4.6. Failure cases

All the methods fail to yield accurate results when evaluated on the “bus” and “guitar” categories, as indicated by the high median errors. After visual inspection (see Figure 7), it appears that 3D models from the guitar category can be very thin under some viewpoints. Moreover, both the guitar and bus categories are ‘almost symmetric’, in the sense that only small details make the pose non-ambiguous.

To check if this is really the reason for the poor performance on these two categories, we re-run the evaluation by taking the reference view for the “guitar” category to be the view with the largest silhouette and by treating both categories as having a 180-degree symmetry. Table 4 presents the results of this new evaluation; the metrics are significantly better. This shows that the failures are indeed caused by views where the objects appear to be very thin, and by ‘quasi-symmetries’.

5. Conclusion

We have presented NOPE, an approach to estimate the pose of novel objects from a single image. Our experiments have shown that direct inference of view embeddings from a single view allows for accurate object pose estimation, even for objects from unseen categories, while requiring neither retraining nor a 3D model. Furthermore, we have evidenced that the template matching approach we follow lets us estimate the pose ambiguities that arise for many objects.

Acknowledgments. We thank Elliot Vincent, Mathis Petrovich and Nicolas Dufour for helpful discussions. This research was produced within the framework of Energy4Climate Interdisciplinary Center (E4C) of IP Paris and Ecole des Ponts ParisTech, and was supported by 3rd *Programme d’Investissements d’Avenir* [ANR-18-EUR-0006-02] and by the Foundation of Ecole polytechnique (Chaire “Défis Technologiques pour une Énergie Responsable” financed by TotalEnergies). This work was performed using HPC resources from GENCI–IDRIS 2022-AD011012294R2.

References

- [1] Seungryul Baek, Kwang In Kim, and Tae-Kyun Kim. Weakly-Supervised Domain Adaptation via GAN and Mesh Model for Estimating 3D Hand Poses Interacting Objects. In *Conference on Computer Vision and Pattern Recognition*, 2020. 1
- [2] Vassileios Balntas, Andreas Doumanoglou, Caner Sahin, Juil Sock, Rigas Kouskouridas, and Tae-Kyun Kim. Pose Guided RGBD Feature Learning for 3D Object Pose Estimation. In *International Conference on Computer Vision*, 2017. 3
- [3] Angel X. Chang, Thomas Funkhouser, Leonidas Guibas, Pat Hanrahan, Qixing Huang, Zimo Li, Silvio Savarese, Manolis Savva, Shuran Song, Hao Su, and Others. ShapeNet: An Information-Rich 3D Model Repository. In *arXiv Preprint*, 2015. 5
- [4] Maximilian Denninger, Martin Sundermeyer, Dominik Winkelbauer, Youssef Zidan, Dmitry Olefir, Mohamad Elbadrawy, Ahsan Lodhi, and Harinandan Katam. BlenderProc. In *arXiv Preprint*, 2019. 5
- [5] Alexander Grabner, Peter M. Roth, and Vincent Lepetit. 3D Pose Estimation and 3D Model Retrieval for Objects in the Wild. In *Conference on Computer Vision and Pattern Recognition*, 2018. 2
- [6] Xingyi He, Jiaming Sun, Yuang Wang, Di Huang, Hujun Bao, and Xiaowei Zhou. OnePose++: Keypoint-Free One-Shot Object Pose Estimation Without CAD Models. In *Advances in Neural Information Processing Systems*, 2022. 1
- [7] Jonathan Ho, Ajay Jain, and Pieter Abbeel. Denoising Diffusion Probabilistic Models. In *Advances in Neural Information Processing Systems*, 2020. 2
- [8] Yinlin Hu, Joachim Hugonot, Pascal Fua, and Mathieu Salzmann. Segmentation-Driven 6D Object Pose Estimation. In *Conference on Computer Vision and Pattern Recognition*, 2019. 1
- [9] Ajay Jain, Ben Mildenhall, Jonathan T. Barron, Pieter Abbeel, and Ben Poole. Zero-Shot Text-Guided Object Generation with Dream Fields, 2022. 2
- [10] Ajay Jain, Amber Xie, and Pieter Abbeel. VectorFusion: Text-to-SVG By Abstracting Pixel-Based Diffusion Models. In *ACM SIGGRAPH*, 2022. 2
- [11] Hanwen Jiang, Zhenyu Jiang, Kristen Grauman, and Yuke Zhu. Few-View Object Reconstruction with Unknown Categories and Camera Poses. In *arXiv Preprint*, 2022. 5
- [12] Wadim Kehl, Fabian Manhardt, Federico Tombari, Slobodan Ilic, and Nassir Navab. SSD-6D: Making RGB-Based 3D Detection and 6D Pose Estimation Great Again. In *International Conference on Computer Vision*, 2017. 1
- [13] Nasir Mohammad Khalid, Tianhao Xie, Eugene Belilovsky, and Popa Tiberiu. CLIP-Mesh: Generating Textured Meshes from Text Using Pretrained Image-Text Models. In *ACM SIGGRAPH*, 2022. 2
- [14] Yann Labbé, Justin Carpentier, Mathieu Aubry, and Josef Sivic. CosyPose: Consistent Multi-View Multi-Object 6D Pose Estimation. In *European Conference on Computer Vision*, 2020. 1, 3
- [15] Yann Labbé, Lucas Manuelli, Arsalan Mousavian, Stephen Tyree, Stan Birchfield, Jonathan Tremblay, Justin Carpentier, Mathieu Aubry, Dieter Fox, and Josef Sivic. MegaPose: 6D Pose Estimation of Novel Objects via Render & Compare. In *CoRL*, 2022. 1, 3
- [16] Yi Li, Gu Wang, Xiangyang Ji, Yu Xiang, and Dieter Fox. DeepIM: Deep Iterative Matching for 6D Pose Estimation. In *European Conference on Computer Vision*, 2018. 1
- [17] Chen-Hsuan Lin, Jun Gao, Luming Tang, Towaki Takikawa, Xiaohui Zeng, Xun Huang, Karsten Kreis, Sanja Fidler, Ming-Yu Liu, and Tsung-Yi Lin. Magic3D: High-Resolution Text-to-3D Content Creation. In *arXiv Preprint*, 2022. 2
- [18] Yuan Liu, Yilin Wen, Sida Peng, Cheng Lin, Xiaoxiao Long, Taku Komura, and Wenping Wang. Gen6D: Generalizable Model-Free 6DoF Object Pose Estimation from RGB Images. In *European Conference on Computer Vision*, 2022. 3
- [19] Ilya Loshchilov and Frank Hutter. Decoupled Weight Decay Regularization. In *International Conference for Learning Representations*, 2019. 6
- [20] Fabian Manhardt, Diego Martin Arroyo, Christian Rupprecht, Benjamin Busam, Tolga Birdal, Nassir Navab, and Federico Tombari. Explaining the Ambiguity of Object Detection and 6D Pose From Visual Data. In *International Conference on Computer Vision*, 2019. 2
- [21] Octave Mariotti, Oisín Mac Aodha, and Hakan Bilen. ViewNet: Unsupervised Viewpoint Estimation from Conditional Generation. In *International Conference on Computer Vision*, 2021. 5, 6, 8
- [22] Octave Mariotti and Hakan Bilen. Semi-Supervised Viewpoint Estimation with Geometry-aware Conditional Generation. In *ECCV Workshop*, 2020. 3, 5, 6, 8
- [23] Octave Mariotti, Oisín Mac Aodha, and Hakan Bilen. ViewNeRF: Unsupervised Viewpoint Estimation Using Category-Level Neural Radiance Fields. In *British Machine Vision Conference*, 2022. 3
- [24] Luke Melas-Kyriazi, Christian Rupprecht, Iro Laina, and Andrea Vedaldi. RealFusion: 360° Reconstruction of Any Object from a Single Image. In *arXiv Preprint*, 2023. 2
- [25] Ben Mildenhall, Pratul P. Srinivasan, Matthew Tancik, Jonathan T. Barron, Ravi Ramamoorthi, and Ren Ng. Nerf: Representing Scenes as Neural Radiance Fields for View Synthesis. In *European Conference on Computer Vision*, 2020. 2, 8
- [26] Thomas Müller, Alex Evans, Christoph Schied, and Alexander Keller. Instant Neural Graphics Primitives with a Multiresolution Hash Encoding. *IEEE Transactions on Robotics and Automation*, 41(4), July 2022. arXiv:2201.05989 [cs]. 2

- [27] Van Nguyen Nguyen, Yuming Du, Yang Xiao, Michael Ramamonjisoa, and Vincent Lepetit. PIZZA: A Powerful Image-only Zero-Shot Zero-CAD Approach to 6 DoF Tracking. In *International Conference on 3D Vision*, 2022. 2, 5, 6, 7, 8
- [28] Van Nguyen Nguyen, Yinlin Hu, Yang Xiao, Mathieu Salzmann, and Vincent Lepetit. Templates for 3D Object Pose Estimation Revisited: Generalization to New Objects and Robustness to Occlusions. In *Conference on Computer Vision and Pattern Recognition*, 2022. 2, 3, 4, 5
- [29] Markus Oberweger, Mahdi Rad, and Vincent Lepetit. Making Deep Heatmaps Robust to Partial Occlusions for 3D Object Pose Estimation. In *European Conference on Computer Vision*, 2018. 1
- [30] Sida Peng, Yuan Liu, Qixing Huang, Xiaowei Zhou, and Hujun Bao. PVNet: Pixel-Wise Voting Network for 6DoF Pose Estimation. In *Conference on Computer Vision and Pattern Recognition*, 2019. 1, 3
- [31] Giorgia Pitteri, Aurélie Bugeau, Slobodan Ilic, and Vincent Lepetit. 3D Object Detection and Pose Estimation of Unseen Objects in Color Images with Local Surface Embeddings. In *Asian Conference on Computer Vision*, 2020. 2, 3
- [32] Ben Poole, Ajay Jain, Jonathan T. Barron, and Ben Mildenhall. DreamFusion: Text-to-3D Using 2D Diffusion. In *arXiv Preprint*, 2022. 2
- [33] Mahdi Rad and Vincent Lepetit. BB8: A Scalable, Accurate, Robust to Partial Occlusion Method for Predicting the 3D Poses of Challenging Objects Without Using Depth. In *International Conference on Computer Vision*, 2017. 1
- [34] Alec Radford, Jong Wook Kim, Chris Hallacy, Aditya Ramesh, Gabriel Goh, Sandhini Agarwal, Girish Sastry, Amanda Askell, Pamela Mishkin, Jack Clark, Gretchen Krueger, and Ilya Sutskever. Learning Transferable Visual Models From Natural Language Supervision. In *International Conference on Machine Learning*, 2021. 2
- [35] Aditya Ramesh, Prafulla Dhariwal, Alex Nichol, Casey Chu, and Mark Chen. Hierarchical Text-Conditional Image Generation with CLIP Latents. In *arXiv Preprint*, 2022. 2
- [36] Robin Rombach, Andreas Blattmann, Dominik Lorenz, Patrick Esser, and Björn Ommer. High-Resolution Image Synthesis with Latent Diffusion Models. In *Conference on Computer Vision and Pattern Recognition*, 2022. 3
- [37] Nataniel Ruiz, Yuanzhen Li, Varun Jampani, Yael Pritch, Michael Rubinstein, and Kfir Aberman. DreamBooth: Fine Tuning Text-To-Image Diffusion Models for Subject-Driven Generation. In *arXiv Preprint*, 2022. 2
- [38] Chitwan Saharia, William Chan, Saurabh Saxena, Lala Li, Jay Whang, Emily Denton, Seyed Kamyar Seyed Ghasemipour, Burcu Karagol Ayan, S. Sara Mahdavi, Rapha Gontijo Lopes, and Others. Photorealistic Text-to-Image Diffusion Models with Deep Language Understanding. In *arXiv Preprint*, 2022. 2
- [39] Katja Schwarz, Axel Sauer, Michael Niemeyer, Yiyi Liao, and Andreas Geiger. VoxGRAF: Fast 3D-Aware Image Synthesis with Sparse Voxel Grids. In *arXiv Preprint*, 2022. 2
- [40] Ivan Shugurov, Fu Li, Benjamin Busam, and Slobodan Ilic. OSOP: A Multi-Stage One Shot Object Pose Estimation Framework. In *Conference on Computer Vision and Pattern Recognition*, 2022. 2, 3
- [41] Jiaming Song, Chenlin Meng, and Stefano Ermon. Denoising Diffusion Implicit Models. In *International Conference for Learning Representations*, 2021. 2
- [42] Yongzhi Su, Mahdi Saleh, Torben Fetzner, Jason Rambach, Nassir Navab, Benjamin Busam, Didier Stricker, and Federico Tombari. ZebraPose: Coarse to Fine Surface Encoding for 6 DoF Object Pose Estimation. In *Conference on Computer Vision and Pattern Recognition*, 2022. 3
- [43] Jiaming Sun, Zihao Wang, Siyu Zhang, Xingyi He, Hongcheng Zhao, Guofeng Zhang, and Xiaowei Zhou. OnePose: One-Shot Object Pose Estimation Without CAD Models. In *Conference on Computer Vision and Pattern Recognition*, 2022. 1, 2, 3
- [44] Martin Sundermeyer, Maximilian Durner, En Yen Puang, Zoltan-Csaba Marton, Narunas Vaskevicius, Kai O. Arras, and Rudolph Triebel. Multi-Path Learning for Object Pose Estimation Across Domains. In *Conference on Computer Vision and Pattern Recognition*, 2020. 1, 2, 3
- [45] Martin Sundermeyer, Zoltan-Csaba Marton, Maximilian Durner, Manuel Brucker, and Rudolph Triebel. Implicit 3D Orientation Learning for 6D Object Detection from RGB Images. In *European Conference on Computer Vision*, 2018. 3
- [46] Martin Sundermeyer, Zoltan-Csaba Marton, Maximilian Durner, and Rudolph Triebel. Augmented Autoencoders: Implicit 3D Orientation Learning for 6D Object Detection. *International Journal of Computer Vision*, 128(3), 2020. 1
- [47] Bugra Tekin, Sudipta N. Sinha, and Pascal Fua. Real-Time Seamless Single Shot 6D Object Pose Prediction. In *Conference on Computer Vision and Pattern Recognition*, 2018. 1
- [48] Jonathan Tremblay, Thang To, Balakumar Sundaralingam, Yu Xiang, Dieter Fox, and Stan Birchfield. Deep Object Pose Estimation for Semantic Robotic Grasping of Household Objects. In *Conference on Robot Learning (CoRL)*, 2018. 1
- [49] B. Ummenhofer, H. Zhou, J. Uhrig, N. Mayer, Eddy Ilg, Alexey Dosovitskiy, and Thomas Brox. Demon: Depth and Motion Network for Learning Monocular Stereo. In *Conference on Computer Vision and Pattern Recognition*, 2017. 2
- [50] Yael Vinker, Ehsan Pajouheshgar, Jessica Y. Bo, Roman Christian Bachmann, Amit Haim Bermano, Daniel Cohen-Or, Amir Zamir, and Ariel Shamir. CLIPasso: Semantically-Aware Object Sketching. In *ACM SIGGRAPH*, 2022. 2
- [51] He Wang, Srinath Sridhar, Jingwei Huang, Julien Valentin, Shuran Song, and Leonidas J. Guibas. Normalized Object Coordinate Space for Category-Level 6D Object Pose and Size Estimation. In *Conference on Computer Vision and Pattern Recognition*, 2019. 2
- [52] Daniel Watson, William Chan, Ricardo Martin-Brualla, Jonathan Ho, Andrea Tagliasacchi, and Mohammad Norouzi. Novel View Synthesis with Diffusion Models. In *International Conference for Learning Representations*, 2023. 2, 3, 5, 6, 8

- [53] Paul Wohlhart and Vincent Lepetit. Learning Descriptors for Object Recognition and 3D Pose Estimation. In *Conference on Computer Vision and Pattern Recognition*, 2015. 3
- [54] Dejjia Xu, Yifan Jiang, Peihao Wang, Zhiwen Fan, Yi Wang, and Zhangyang Wang. NeuralLift-360: Lifting An In-the-wild 2D Photo to A 3D Object with 360° Views. In *Conference on Computer Vision and Pattern Recognition*, 2022. 2
- [55] Alex Yu, Sara Fridovich-Keil, Matthew Tancik, Qinhong Chen, Benjamin Recht, and Angjoo Kanazawa. Plenoxels: Radiance Fields Without Neural Networks. In *Conference on Computer Vision and Pattern Recognition*, 2022. 2
- [56] Alex Yu, Vickie Ye, Matthew Tancik, and Angjoo Kanazawa. pixelNeRF: Neural Radiance Fields from One or Few Images. In *Conference on Computer Vision and Pattern Recognition*, 2021. 2
- [57] Sergey Zakharov, Ivan S. Shugurov, and Slobodan Ilic. DPOD: 6D Pose Object Detector and Refiner. In *International Conference on Computer Vision*, 2019. 1
- [58] Jason Y. Zhang, Deva Ramanan, and Shubham Tulsiani. RelPose: Predicting Probabilistic Relative Rotation for Single Objects in the Wild. In *European Conference on Computer Vision*, 2022. 1, 2, 3
- [59] Chen Zhao, Yinlin Hu, and Mathieu Salzmann. Fusing Local Similarities for Retrieval-based 3D Orientation Estimation of Unseen Objects. In *European Conference on Computer Vision*, 2022. 3
- [60] Zhun Zhong, Liang Zheng, Guoliang Kang, Shaozi Li, and Yi Yang. Random erasing data augmentation. In *AAAI*, 2020. 6
- [61] Yi Zhou, Connelly Barnes, Jingwan Lu, Jimei Yang, and Hao Li. On the continuity of rotation representations in neural networks. In *Proceedings of the IEEE/CVF Conference on Computer Vision and Pattern Recognition*, pages 5745–5753, 2019. 8
- [62] Zhizhuo Zhou and Shubham Tulsiani. SparseFusion: Distilling View-conditioned Diffusion for 3D Reconstruction. In *arXiv Preprint*, 2023. 2